(Preprint) AAS 24-375

REACTION WHEEL MOMENTUM CONTROL WHILE ELECTROSTATICALLY TUGGING SPACE OBJECT

James D. Walker III[*], Kaylee Champion[†], and Hanspeter Schaub[‡]

Charged spacecraft generate electrostatic forces and torques on one another. This can be a threat to long-term servicing missions as a constant external torque causes reaction wheels to continually increase in speed in order to store the additional angular momentum. The electrostatic tractor is one such mission concept. It requires both the servicer and target to have 10's of kilovolt potentials and maintain a 10-15 m separation distance. By utilizing the electrostatic force between the two spacecraft, the servicer tugs the debris to a graveyard orbit. However, due to the large potentials and small separation distance, the servicer experiences significant electrostatic torques that may eventually cause the reaction wheels to saturate. A method for managing the angular momentum of the servicer using the same electrostatic torques is presented here. By rotating the servicer to attitudes where electrostatic torques act opposite each other, the angular momentum of a servicer can be decreased without additional fuel or instruments. Using this technique, it is shown that the angular momentum of a servicer can be driven from 350 Nms to approximately zero in about 15 hours. It is also shown that a servicer can repeatedly rotate between two attitudes with opposing electrostatic torques to keep its angular momentum from continually increasing and extend the lifetime of the mission. For the simple scenario described here, maintaining the servicing attitude causes the servicer's reaction wheels to saturate in 39,000 s. Employing electrostatic momentum management is shown to increase this saturation time to over 250,000 s, extending the lifetime of the servicing spacecraft.

INTRODUCTION

The space environment is not truly empty. Populations of electrons, protons, ions, and photons are expelled from the Sun as solar wind and travel throughout the solar system. When conducting spacecraft are exposed to these energetic particles, the interactions lead to spacecraft charging, where the electric potential of the satellite deviates from that of the surrounding plasma.[1] For isolated spacecraft, differential charging is a concern: if a satellite's outer surface is not fully conducting, different components can have different electric potentials which leads to electrostatic discharges between the components. For neighboring spacecraft however, the effects of spacecraft charging are more complicated. Two charged bodies exert Coulomb forces and torques on one-another that increase exponentially as their separation distance decreases. As two charged spacecraft approach one-another, these forces and torques influence the relative motion of the two spacecraft, decreasing

[*]NDSEG Fellow, Ann and H.J. Smead Department of Aerospace Engineering Sciences, University of Colorado Boulder, Colorado Center for Astrodynamics Research, Boulder, CO, 80303 USA. James.WalkerIii@colorado.edu

[†]NSTGRO Fellow, Ann and H.J. Smead Department of Aerospace Engineering Sciences, University of Colorado Boulder, Colorado Center for Astrodynamics Research, Boulder, CO, 80303 USA. kaylee.champion@colorado.edu

[‡]Professor and Department Chair, Schaden Leadership Chair, Ann and H.J. Smead Department of Aerospace Engineering Sciences, Colorado Center for Astrodynamics Research. AAS Fellow, AIAA Fellow

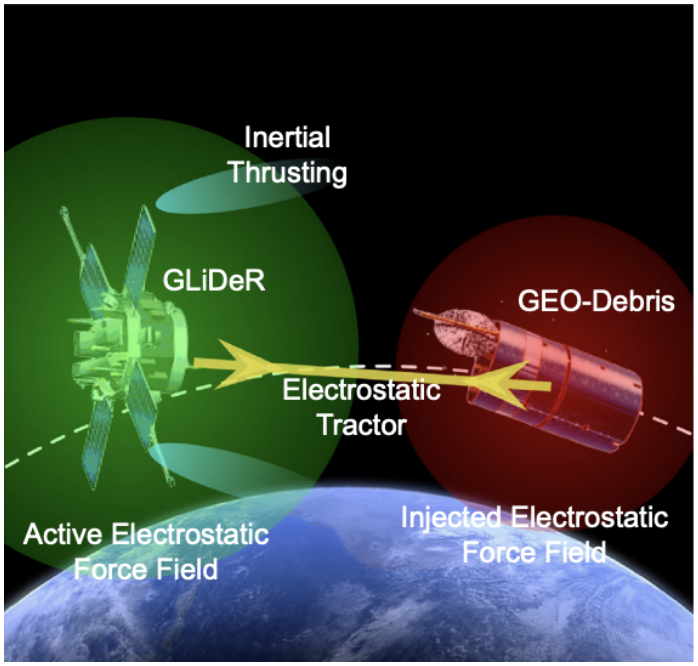

Figure 1. Conceptual representation of a servicer tugging geostationary debris using the Electrostatic Tractor method.[6]

the efficiency of the motion controller and, if the perturbations are large enough, causing a collision.[2–4] Docking operations are especially vulnerable to the effects of spacecraft charging due to small separation distances and physical contact between the two charged objects.[4] When the potentials of docking spacecraft are different, arching can occur and cause damage to both objects.[4] Spacecraft charging and its effects are a significant concern in geostationary and cislunar regions where the hot, dense plasma and eclipsed orbits lead to spacecraft potentials ranging from a few volts positive to tens of thousands of volts negative.[1] These regions also have relatively large Debye lengths (greater than one hundred meters), meaning spacecraft can electrostatically interact across large distances.[1]

Because electrostatic forces and torques are non-contact forces, they offer unique capabilities for debris removal. The electrostatic tractor (ET) is a novel method that utilizes the Coulomb force and torque generated between two charged spacecraft for contactless debris removal.[5–8] The concept is as follows: a servicer equipped with a high energy electron beam directs the stream of electrons at the debris.[6] As the additional negative current charges the target negatively, the expulsion of electrons causes the servicer to charge positively.[6] These opposing charges generate an attractive force that ”connects” the two spacecraft.[6] Using low impulse thrusters, the servicer can then tug the debris to a new orbit, while maintaining a constant separation distance.[7,8] Figure 1 shows concept art of this process. In Ref. 9, it is shown that a multi-ton debris object can be re-orbited over the course of months.[9] The electrostatic tractor is designed to be employed in regions with Debye lengths greater than 10-30 meters and significant spacecraft potentials like geostationary and cislunar orbits.[6]

The translational and attitude dynamics generated by these electrostatic forces have been explored in previous research. Wilson and Schaub explore the impact of electrostatic perturbations on

servicing operations, determining the station keeping requirements for charged spacecraft and the electrostatically perturbed trajectory for a nominal rendezvous mission.[2] The dynamics and control requirements for the proximity operations of the ET have also been extensively explored. In Ref. 10, a relative motion control algorithm is developed and shown to allow a chief spacecraft to increase the semi-major axis of a deputy by 300 km using electrostatic forces. Electrostatic torques are also found to have a significant impact on the attitude of charged spacecraft for separation distances up to of 3-4 spacecraft radii.[11] The generation of significant electrostatic torques between nearby spacecraft led to development of attitude control algorithms for detumbling uncontrolled debris.[11–14] It has been shown using both experiments and numeric simulations that, by controlling the attitude and electrostatic potential of an axis-symmetric servicer, it is possible to detumble a rotating target.[11–15] Because electrostatic torques are internal torques, by detumbling the space debris, the servicer is absorbing the target's angular momentum and storing it in its reaction wheels (RWs). This use of electrostatic torques for angular momentum management of a target also inspired the idea of using them for angular momentum management of the servicer itself.

Servicing missions using the ET can be uniquely affected by spacecraft charging. When a servicer is maintaining a desired attitude relative to a target, each spacecraft experiences a constant torque. Reaction wheels are used to store the increasing angular momentum; however, because these torques are constant, the reaction wheels continually speed up to maintain the desired attitude. Eventually, the wheels will reach a maximum speed, saturate, and the desired attitude will no longer be maintained. To reduce the electrostatic torque experienced during proximity operations, Ref. 3 develops a method for determining the approach trajectory that reduces the torque that the target (and therefore also the servicer) experiences. This technique assumes the target object is not tumbling during the approach.[3] The total change in angular velocity of the target was decreased by 95% using this method compared to directly approaching the target.[3] However, even though the perturbations to the spacecraft attitudes can be reduced, electrostatic torques will still be present between charged spacecraft. To extend the lifetime of long term servicing mission in high altitude orbits, methods for reducing the speed of reaction wheels must be employed. Redundant reaction wheels can be used to increase the amount of angular momentum stored about a particular axis and additional reaction wheels mounted on different axes can allow for angular momentum to be redistributed.[16,17] Eventually, however, the wheels will saturate. Thrusters and magnetorquers have been used to allow reaction wheels to dump momentum and decrease their wheel speeds. Thrusters burn fuel to apply a torque opposite to the angular momentum of the spacecraft[18] while magnetorquers generate a magnetic dipole and interact with Earth's magnetic field to apply an external torque to spin down the reaction wheels.[16,19–21] However, thrusters require additional fuel, magnetorquers are most effective near Earth, and both require additional mass and space.

Rather than adding instruments or using additional fuel, this paper proposes the use of Coulomb torques to maintain reaction wheel speeds. When preforming the ET and similar maneuvers, spacecraft will have electric potentials greater than ten kilovolts and be 2-3 spacecraft radii away from one another ($\approx$15 m);[6] therefore they experience significant electrostatic torques. Because electrostatic torques are internal torques, the overall angular momentum of the system will remain the same throughout the entire operation, but the angular momentum on each spacecraft will not. Instead, it will increase equally in magnitude (but opposite direction) on each spacecraft. Rather than letting the wheels spin up until they saturate, the orientation of the servicer can be adjusted such that angular momentum on each spacecraft will decrease in magnitude. This momentum dumping process of the servicer will naturally transfer the momentum to the debris object, causing the debris

to tumble. Interestingly, References 22 and 23 found that relative position station keeping control for the ET is sensitive to the attitude of stationary debris and certain debris orientations cause the servicer's station keeping control to become unstable. When the debris is rotating, the impact of the three-dimensional shape averages out and these instabilities do not occur.[22] However, rotating targets does introduce other complications such as time varying potentials and attitude dependent solar radiation pressure. The comparison of stationary vs tumbling debris is part of ongoing research.

The electrostatic torques are dependent on the orientation of the servicer relative to the target. For non-symmetric spacecraft, there are orientations where the target applies a positive torque and others where the torque is negative. Starting at a desired reference attitude relative to the target, the reaction wheels of the servicer will spin up. Once they reach a wheel speed threshold (less than the maximum wheel speed), the servicer can compute, and rotate to, the relative orientation that will yields the opposite torque. Holding this attitude, the reaction wheels will spin down and then the servicer will rotate back to the reference attitude. This allows the spacecraft to spin down its reaction wheels using only electrical energy and extend the lifetime of these missions.

The goal of this paper is to introduce the concept of electrostatic momentum transfer and present it for simple and idealized charging scenarios. Specifically, a servicer is equipped with a three-axis control while the target remains at a fixed attitude. This scenario is representative of a servicing spacecraft operating near a target with a large capacity to store angular momentum, such as the International Space Station (ISS) or Lunar Gateway.

The paper is structured as follows: an outline of the reaction wheel control implemented throughout this paper is given first and then followed by the modeling technique for computing the electrostatic torques experienced by each spacecraft. The details of the momentum management technique are presented in the following section. Finally, the results of the reaction wheel momentum control are shown for two scenarios. The first scenario is a single momentum transfer maneuver: a spacecraft with high reaction wheel speeds uses the target to drive its wheel speeds to zero once. The second scenario involves repeated maneuvers. A servicing craft maintaining a desired attitude builds up angular momentum and rotates between the servicing attitude and anti-torque attitude to continually transfer momentum to the target.

NUMERICAL METHODS

Attitude Control

A description of the attitude control used in this paper is given here, but an in depth derivation of the dynamics and control can be found in Chs. 4 and 8 of Ref. 17. Attitude control is only applied to the servicing spacecraft as the target is assumed to be fully controlled and held at a fixed attitude. The attitude control acts independent of translational control; therefore, while translational dynamics are not considered in this paper, they can be added in future work without affecting the attitude control. A reference frame tracking problem is used in the project, where the attitude of the servicer must follow a desired reference. The desired reference varies between two attitudes: the servicing attitude and anti-torque attitude. Reaction wheels are used to apply the control, however adjustments can be made such that other momentum exchange devices are used, such as control moment gyroscopes.[17] The servicer is assumed to be a rigid spacecraft with three reaction wheels mounted with the spin axes aligned with the principle axes of the spacecraft. The numeric values used to define the spacecraft properties used throughout this project are not taken to be those of actual spacecraft, but rather an estimate for large geostationary satellites.

The reaction wheel control law for the RW motor torque set $\boldsymbol{u}_s$ utilizes modified Rodriquez parameters (MRPs) and is given in Ref. 17 as

$$[G_s]\boldsymbol{u}_s = K\boldsymbol{\sigma}_{\text{err}} + P\delta\boldsymbol{\omega} - [\tilde{\boldsymbol{\omega}}]\left([I_{\text{RW}}]\boldsymbol{\omega} + [G_s]\boldsymbol{h}_s\right) - [I_{\text{RW}}]\left(\dot{\boldsymbol{\omega}}_r - \boldsymbol{\omega}\times\boldsymbol{\omega}_r\right) + \boldsymbol{L}_{\text{ext}}. \tag{1}$$

where $\boldsymbol{\omega}$ is the angular velocity of the spacecraft relative to the inertial frame, $\boldsymbol{\omega_r}$ is the angular velocity of the reference frame relative to the inertial frame, $\boldsymbol{\sigma}_{\text{err}}$ is the MRP error between the spacecraft body attitude and reference attitude, and $\delta\boldsymbol{\omega}$ is the angular velocity error between the two attitudes. Both values K and P are adjustable gains and $\boldsymbol{L}_{\text{ext}}$ is the external torque applied to the spacecraft. In this case, only electrostatic torques are considered. Throughout the paper, gains of K = 5 Nm and P = 500 Nms are used.

In Eq. (1), $[G_s]$ is a 3×3 projection matrix that contains the unit direction vectors of the spin axes of the reaction wheels:

$$[G_s] = [\hat{\boldsymbol{g}}_{s_1}, \hat{\boldsymbol{g}}_{s_2}, \hat{\boldsymbol{g}}_{s_3}]. \tag{2}$$

For this paper, the spin axes are aligned with the principle axes of the spacecraft such that their body-fixed $\mathcal{B}$-frame vector components are given by:

$$^{\mathcal{B}}\hat{\boldsymbol{g}}_{s_1} = [1,0,0]^T \tag{3a}$$
$$^{\mathcal{B}}\hat{\boldsymbol{g}}_{s_2} = [0,1,0]^T \tag{3b}$$
$$^{\mathcal{B}}\hat{\boldsymbol{g}}_{s_3} = [0,0,1]^T. \tag{3c}$$

where the sub-subscript corresponds to associated reaction wheel. The vectors shown in Eq. (3) are cast in the body frame of the spacecraft.

The matrix $[I_{\text{RW}}]$ is the inertia matrix of the spacecraft as seen by the body frame and is found by building a CAD model of the servicer and computing the inertial matrix assuming the mass is evenly distributed.[3] Using publicly available documentation, the CAD model is designed for a GOES-R spacecraft, and the momentum of inertia taken to be

$$^{\mathcal{B}}[I_{\text{RW}}] = \begin{bmatrix} 11410 & -70 & 1186 \\ 160 & 22440 & -7260 \\ -468 & 6115 & 26610 \end{bmatrix} \text{kg}\cdot\text{m}^2. \tag{4}$$

While this inertia matrix is not equal to that of the GOES-R spacecraft, it is assumed to be a reasonable estimate for that of a geostationary satellite.

The components of the vector $\boldsymbol{h}_s$ are given by

$$h_{s_i} = I_{W_s}\left(\omega_{s_i} + \Omega_i\right) \tag{5}$$

where i = 1,2,3 corresponding to each reaction wheel. Here, I_{W_s} is the principle inertia of the reaction wheel about its spin axis, ω_{s_i} is the angular velocity of the spacecraft relative to the inertial frame, $\boldsymbol{\omega}$, projected onto the $\hat{\boldsymbol{g}}_{s_i}$ axis, and Ω_i is the wheel speed of reaction wheel i.

Finally, $\boldsymbol{u}_s$ is the motor torque applied to each of the reaction wheels. By solving for $\boldsymbol{u}_s$, the required control is computed and applied to the respective reaction wheels.

Electrostatic Force and Torque Modeling

The external torque considered is the Coulomb torque generated by two charged spacecraft in close proximity to one-another. For simple geometries, such as spheres, computing these torques is relatively simple process. However, for more complex geometries, like those of spacecraft, the problem is much more computationally intensive. Finite element solvers can be used to compute these torques, but they are computationally expensive and are impractical to use for dynamics modeling.[24] Instead, the Multi-Sphere Method (MSM) is employed here.

The MSM is a technique for rapidly computing the electrostatic torques, enabling numerical dynamics modeling with Coulomb forces.[24–27] This computational speed is achieved by discretizing the spacecraft into collections of spheres.[24] The location and radius of each sphere are optimally chosen to match the object shape, and, more importantly, the electric field it generates.[26] Then, by computing the force and torque between each of the spheres and taking the sum, the net force and torque experienced by the spacecraft can be computed.[24] The force/torque calculation between two spheres is much faster than that for more complex shapes; therefore, approximating the spacecraft as a collection of spheres significantly reduces the required computation time.[24] Reference 24 gives a detailed description of the development of the MSM and Ref. 25 outlines the method for selecting the sphere location and size when matching the electrostatic force and torque. The location and radii of the spheres can also be optimized for matching the electric field of the spacecraft for a more robust optimization.[26] It should be noted that this process of discretizing the spacecraft as a set of spheres does require a finite element or method of moments solver; however, this only needs to be computed once for a specific geometry.[24]

The MSM can be implemented to estimate both the electrostatic force and torque applied to the spacecraft, but only the electrostatic torques are of interest for this paper. As such, the method for computing these forces is outlined here, but is presented in Ref. 24.

In order to compute electrostatic torques, the charge on each sphere must be known. This can be computed by exploiting the relationship between charge and voltage. The voltage on an object is dependent on its own charge and the charge of any nearby objects: when two charged bodies are close to one another, there is a coupling effect where the charge of one impacts the charging behavior of the other. Analytic expressions can be used to determine the charge of multibody systems.[24] Equation (6) shows the expression used in the MSM for determining the voltage of a single sphere, V_i:[24]

$$V_i = \frac{1}{4\epsilon_0\pi}\frac{Q_i}{R_i} + \sum_{\substack{k=1 \\ k\neq i}}^{n}\left[\frac{1}{4\epsilon_0\pi}\frac{Q_i}{r_{i,k}}\right]. \tag{6}$$

Here, R_i is the radius of sphere i, Q_i is the charge of sphere i, and $r_{i,k}$ is the separation distance between spheres i and k. Additionally, ϵ_0 is the permeability of free space. Equation (6) can be then be expanded into matrix form for n spheres:

$$\begin{bmatrix} V_1 \\ V_2 \\ \vdots \\ V_n \end{bmatrix} = \underbrace{\frac{1}{4\epsilon_0\pi}\begin{bmatrix} \frac{1}{R_1} & \frac{1}{r_{1,2}} & \cdots & \frac{1}{r_{1,n}} \\ \frac{1}{r_{2,1}} & \frac{1}{R_2} & \cdots & \frac{1}{r_{2,n}} \\ \vdots & \vdots & \ddots & \vdots \\ \frac{1}{r_{n,1}} & \frac{1}{r_{n,2}} & \cdots & \frac{1}{R_n} \end{bmatrix}}_{S} \begin{bmatrix} Q_1 \\ Q_2 \\ \vdots \\ Q_n \end{bmatrix} \tag{7}$$

where S is the elastance matrix. With this relationship, if the location, size, and voltage of each of there spheres is known, the charge on each sphere can be computed.[24] The spacecraft are assumed to be fully conducting, therefore the voltage of each of the spheres is equal to the voltage of the spacecraft. The size and location of each of the spheres is determined during the discretization process.

Now that the charge on each sphere is found, the electrostatic torques between the two bodies can be computed. The total torque about the center of mass experience by a spacecraft is the sum of the torques experience by each sphere as shown by Eq. (8):

$$\boldsymbol{L}_O = \frac{1}{4\epsilon_0 \pi} \sum_{j=1}^{n_T} q_j \sum_{i=1}^{n_S} \left[\frac{q_i}{r_{i,j}^3} \boldsymbol{r}_i \times \boldsymbol{r}_{i,j} \right]. \tag{8}$$

Each of these spacecraft consists of a collection of a different number of spheres. Therefore, n_T denotes the number of spheres representing the target spacecraft while n_S denotes the number of spheres representing the servicer. The variable $\boldsymbol{r}_i$, denotes the distance vector from the center of sphere i to the center of mass of the spacecraft body and $\boldsymbol{r}_{i,j}$ is the distance vector between i-th sphere of the target and the j-th sphere of servicer. The rest of the variables here are the same as define previously. Because q_j does not depend on i, it can be separated from the rest of the summation. The cross product is taken between $\boldsymbol{r}_i$ and $\boldsymbol{r}_{i,j}$ such that the computed torque is about the center of mass of the spacecraft, denoted by the subscript O.

To calculate the electrostatic torques, the center of mass location in the spacecraft's body frame is needed. The servicing spacecraft is chosen to be the GOES-R spacecraft. Because the spacecraft is non-symmetric with a single solar panel and a thin boom, significant electrostatic torques will be generated between it and the target object. Given below is the dry mass of this spacecraft and the inertial Cartesian location of the center of mass estimated using the CAD model:

$$m_s = 2857 \text{ kg} \tag{9}$$

$$CM_s = \left[-2.7993, -0.0552, 0.6477\right] \text{ m}. \tag{10}$$

The target spacecraft is chosen to be the SSL-1300 satellite bus. This spacecraft was chosen as the target due to its large solar panels and symmetric shape. Because the target shape is symmetric, the charge distribution will also be relatively symmetric as shown in Fig. 2. The mass and Cartesian center of mass location in the inertial frame of the SSL-1300 spacecraft bus are

$$m_t = 2000 \text{ kg} \tag{11}$$

$$CM_t = \left[0, 0, 0\right] \text{ m}. \tag{12}$$

Figure 2 shows the MSM representation of these two spacecraft. The GOES-R spacecraft is made up of 80 spheres while the the SSL-1300 spacecraft is made of 108 spheres. A center of mass separation of 15 m is used throughout this project. The largest charge densities occur at the tips of the solar panels and the end up the magnetometer (the thin rod on the GOES-R spacecraft). These regions are thin compared to the rest of spacecraft, but have the same potential, leading to the increased charged density. Interactions between these charge dense regions contribute the most to the electrostatic torque.

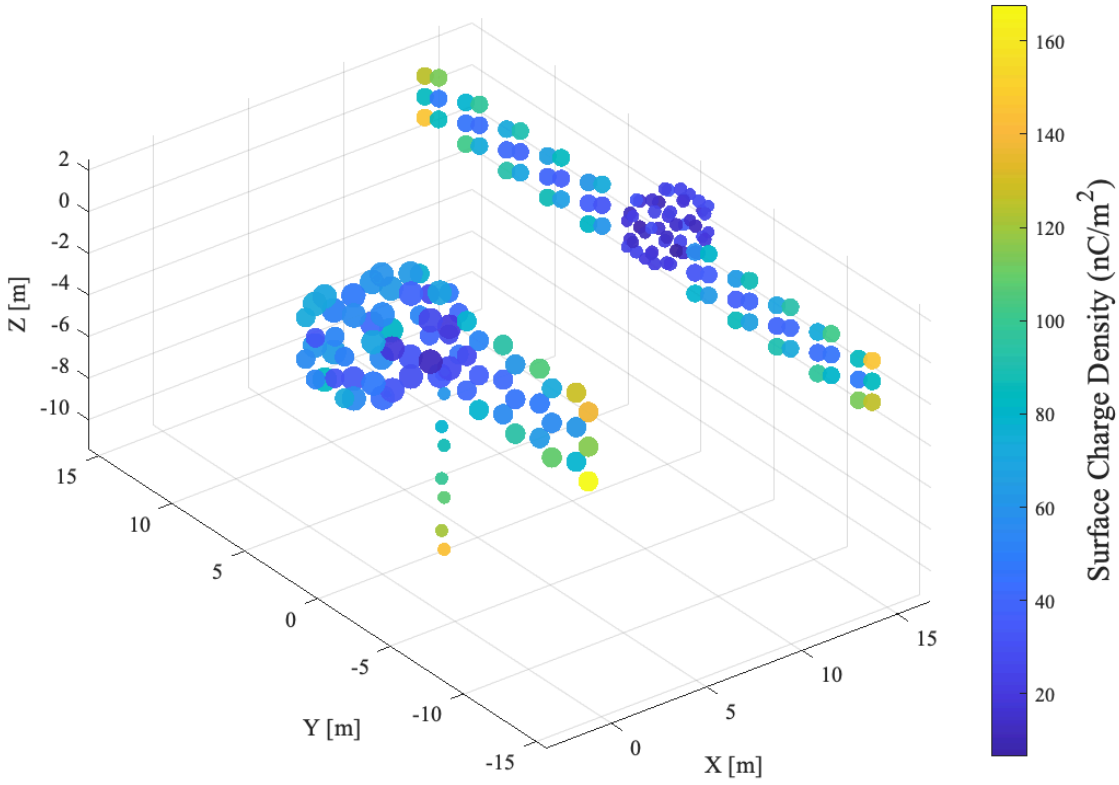

Figure 2. The MSM representation of the GOES-R and SSL-1300 spacecraft for spacecraft potentials of +10 kV and separation distance of 15 m.

Electrostatic Momentum Transfer

The driving idea behind this momentum management method is using torques to decrease the angular momentum of a spacecraft. The derivative of angular momentum $\boldsymbol{H}$ is given by Eq. (13):[17]

$$\dot{\boldsymbol{H}}_P = \boldsymbol{L}_P + M\ddot{\boldsymbol{R}}_P \times (\boldsymbol{R}_c - \boldsymbol{R_P}) \,. \tag{13}$$

Angular momentum and torque must be defined about some point. In Eq. (13), they are defined about an arbitrary point P denoted by the subscript. In the second term, M is mass of the spacecraft, while $\boldsymbol{R}_c$ and $\boldsymbol{R}_P$ are the vectors defining the location of the center of mass and point P, respectively, relative to the origin. In this paper, the origin is taken to be the center of mass of the target and the torques are computed about the same point. This means $\boldsymbol{R}_c = \boldsymbol{R}_P = \boldsymbol{0}_{3\times1}$. With this, Eq. (13) becomes $\dot{\boldsymbol{H}} = \boldsymbol{L}$. The subscripts from Eq. (13) are dropped for the rest of the paper as angular momentum and torque are computed about the origin. The full derivation of Eq. (13) is given in Ch. 2 of Ref. 17.

Equation (13) shows that applying an external torque causes the angular momentum of the spacecraft to change. It should be noted that electrostatic torques are internal relative to the two spacecraft system, but external to the individual spacecraft. Applying these torques can increase/decrease the angular momentum of each spacecraft, but not the overall system angular momentum. While the servicing attitude is maintained, the associated $\boldsymbol{L}_{\text{ext}}$ increases the magnitude of the angular momentum. However, if the servicer rotates to another attitude, the applied $\boldsymbol{L}_{\text{ext}}$ is different and the

angular momentum will change accordingly. By rotating to an attitude where the torque is such that $\boldsymbol{L} = -\boldsymbol{L}_{\text{ext}}$, the angular momentum will decrease at the same rate it increased. In fact, each component $\boldsymbol{H}$ will decrease at the same rate they increased at, meaning maintaining this attitude will result in the angular momentum being driven to zero. Even if the torques are not exactly equal in magnitude, as long as they are perfectly anti-parallel, the angular momentum can be driven to zero. If the torques are not perfectly opposite, the components of the angular momentum vector will reach zero at different times and a zero angular momentum can not be achieved. Therefore, a numerical approach for reliably determine this opposite torque location is developed.

By taking the MSM representations of each spacecraft and computing the torque at a variety of servicer attitudes, a database of the possible electrostatic torques experienced by the spacecraft is built. To develop this database, 3-2-1 Euler Angles are used to represent the attitude. These 3-2-1 Euler Angles can be used to describe any possible attitude with the first and third angles ranging from 0° to 180° and the second angle ranges from ±90°. Each of these ranges are discretized into 100 equally spaced points and the electrostatic torque at every combination of yaw, pitch, and roll angles is computed, giving one million different orientations and torques. This database only needs to be computed once for a given separation distance, electric potential, and set of spacecraft models. Next, the torque experienced at the servicing attitude is compared to each torque in the database: the magnitude of the sum of two torques is computed. The sum of two torques that are directly opposite each other will have a zero magnitude; therefore, finding the minimum magnitude of this pairwise sum will yield the orientation that generates the most anti-parallel electrostatic torque.

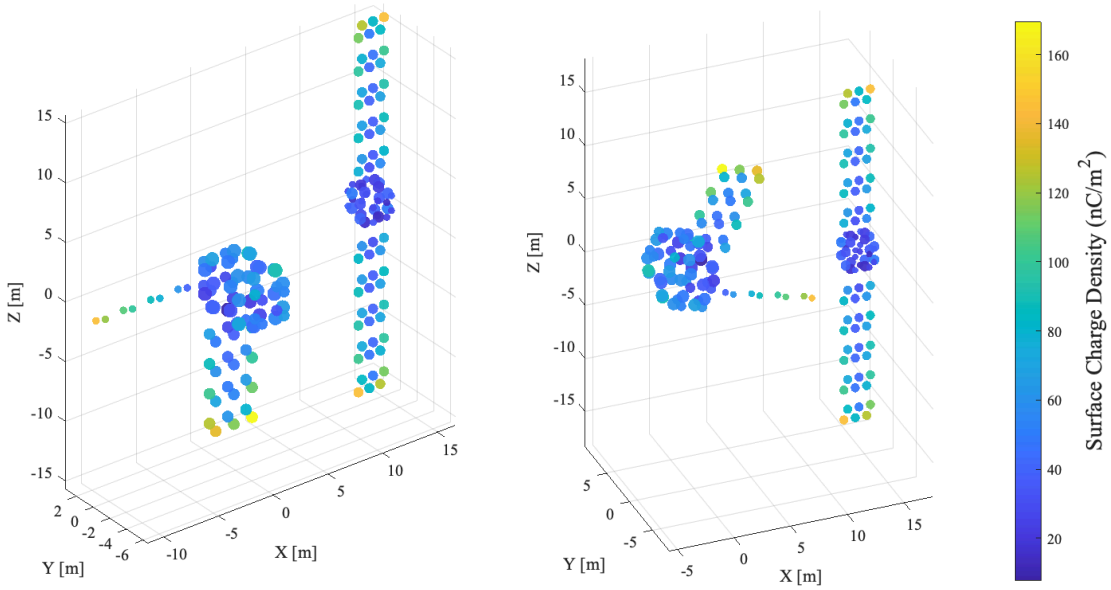

(a) The MSM representation for a servicer attitude of $\boldsymbol{\sigma}$ = (0,0,0).

(b) The MSM representation for a servicer attitude of $\boldsymbol{\sigma}$ = (0.36,0.62,-0.47).

Figure 3. The MSM of the GOES-R and SSL-1300 spacecraft at two altitudes with opposite electrostatic torques. There is a 15 m separation distance between the two spacecraft and they both have an electric potential of 10 kV.

One important note when finding the anti-torque attitude is that, because angular momentum and

electrostatic torque are vectors, they must be expressed in a specific reference frame. In this paper, there are two frames considered, the servicer body frame and the target body frame. Because the target is fixed, its body frame also corresponds to the inertial frame, but the servicer body frame rotates with the spacecraft. To take the sum of these torques torques, they must both be expressed in the same frame. Additionally, when the electrostatic toque is applied to the attitude control, in has to be expressed in the body frame of the spacecraft, in this case the servicer.

Figure 3 shows the servicer/target MSM configurations for the servicing attitude, Fig. 3(a), and anti-torque attitude, Fig. 3(b). At the serving attitude, the servicer experiences an electrostatic torque of ${}^{\mathcal{B}}\boldsymbol{L}_e$ = [0.0003, -0.0026, 0.0018]$^{\mathrm{T}}$ Nm. Once the servicer's reaction wheels spin up, it rotates to the anti-torque attitude, where the electrostatic torque is ${}^{\mathcal{B}}\boldsymbol{L}_e$ = [-3.9e-5 ,0.0027, -0.0021]$^{\mathrm{T}}$ Nm. Both these torques are expressed in the inertial frame. Normalizing these two vectors and taking the dot product gives a value of -0.995. For perfectly opposite vectors, this value is -1, therefore a value of -0.995 indicates that, while it is not perfect, these two vectors are very close to anti-parallel.

RESULTS

Single Momentum Management Maneuver with a Fixed Target

Before exploring continuous momentum management for a servicing mission, a single momentum management maneuver is conducted. The spacecraft scenario is as follows: an independent spacecraft has absorbed significant angular momentum with its reaction wheels. This may have been caused by proximity operations between charged spacecraft, solar radiation pressure, or another mechanism. With significant angular momentum stored in the reaction wheels, the spacecraft must reduce the associated large wheel speeds. In this case, it uses electrostatic torques to transfer the momentum to a controlled target spacecraft. Knowing the geometry and electric potential of both spacecraft, the servicer computes the relative attitude that results in a torque opposite to its angular momentum. The servicer maintains this attitude until its angular momentum reaches zero (or until it stops decreasing in magnitude).

The servicer is a GOES-R spacecraft with an electrostatic potential of $+10$ kV and an initial angular momentum (expressed in the servicer's body frame components) of ${}^{\mathcal{B}}\boldsymbol{H}_0$ = [280, -210, 3.5]$^{\mathrm{T}}$ Nms, shown by the red arrow in Fig. 4. In this case, the target has a zero angular velocity relative to the inertial frame, therefore the angular momentum is entirely stored in the servicer's reaction wheels. A $+10$ kV potential is also prescribed to the stationary target, the SSL-1300 spacecraft bus. This results in a constant repulsive electrostatic torque applied to both spacecraft. Using the process described previously, the electrostatic torque that drives the servicer's angular momentum to zero is ${}^{\mathcal{B}}\boldsymbol{L}_e$ = [0.0052, 0.0039, 6.5e-5]$^{\mathrm{T}}$ Nm, shown by the blue arrow. The dot product between the normalized angular momentum and normalized electrostatic torque is equal to -1.0, indicating the two vectors are nearly anti-parallel. A maximum torque output is taken to be 0.1 Nm, which can be achieved by large reaction such as the Honeywell HR14.[28] Additionally, I_{W_s} is taken to be 1 and all the wheels are assumed to be identical.

Figure 5 shows the magnitude of the angular momentum of the servicer as well as the speeds of its reaction wheels. It can be seen that, as the servicer maintains this attitude, the reaction wheel speeds steadily decrease until they all reach approximately zero at the same time. The same behavior can be seen for the angular momentum of the servicer. This is expected as the angular momentum is determined by the reaction wheels. It takes 54,140 seconds or just over 15 hours of maintaining this attitude for the angular momentum to reach a minimum magnitude of 0.031 Nms. This value does

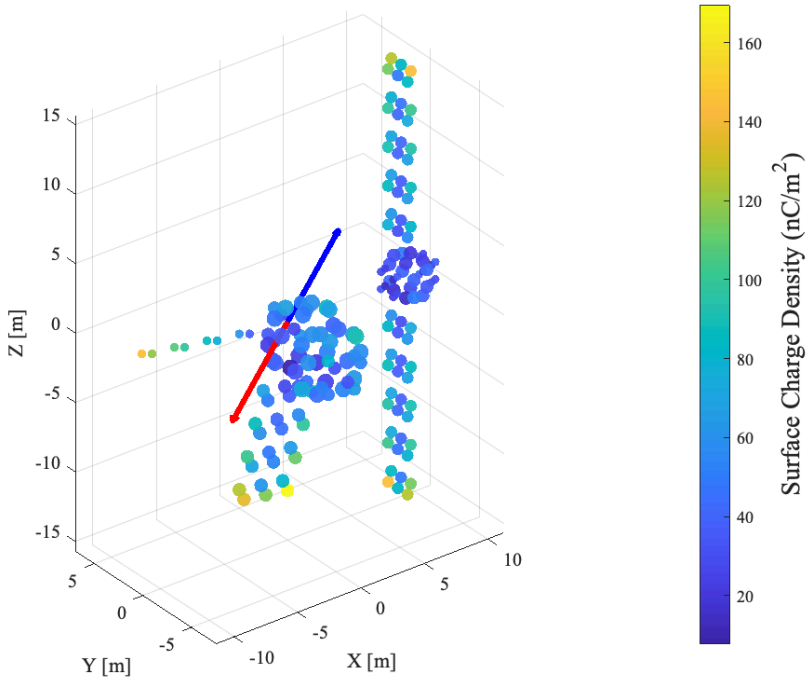

Figure 4. The MSM representation of the GOES-R with a non-zero initial angular momentum and SSL-1300 spacecraft. Here, the red vector indicates the initial angular momentum vector of the servicer while the blue indicates the electrostatic torque generated by the spacecraft. Magnitudes of these vector are not to scale.

not reach exactly zero as the torque and angular momentum vector are not perfectly anti-parallel.

The results shown in Fig. 5 show the momentum transfer when the computed electrostatic torque is nearly anti-parallel to the servicer's initial angular momentum vector. However, there is not a guarantee that this perfect torque can be found. In fact, most of the computed anti-torque vectors have a significant non-anti-parallel component because the database has a resolution of approximately 1.8°.

A similar scenario to that presented by Fig. 4 is shown in Fig. 6 only now the electrostatic torque has a more significant non-anti-parallel component. The applied electrostatic torque here is ${}^{B}\boldsymbol{L}_e$ = [0.0098, 0.0035, 3.2e-5]$^{\mathrm{T}}$ Nm. Taking the normalized dot product between the angular momentum vector and this new torque vector gives a value of -0.95, meaning the electrostatic torque still acts relatively opposite to the initial angular momentum vector. This represents an extreme case and could be resolved in future simulations by generating a more finely resolved database. However, this scenario clearly illustrates the effect of the resolution of the database.

It can be seen in Fig. 6(a) that the reaction wheels reach a zero velocity at different times. The X axis reaction wheel achieves this at 28,480 s while the Y axis reaction wheel takes the full 60,000 s seconds to reach a near zero velocity. This difference causes the two major features of Fig. 6(b): the parabolic shape and non-zero minimum. Because the velocity of the Z axis reaction wheel is 2 orders of magnitude smaller than the others, it does not have a significant effect on the overall behavior of the spacecraft.

When the the reaction wheel speeds reach 0 rad/s at the same time, the rate of change of the

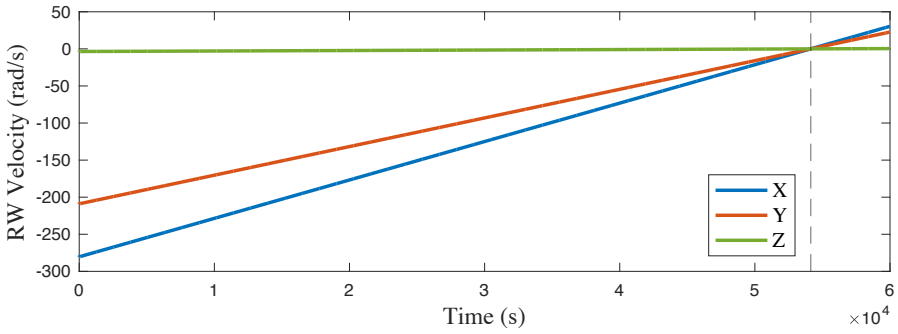

(a) Servicer reaction wheel velocities.

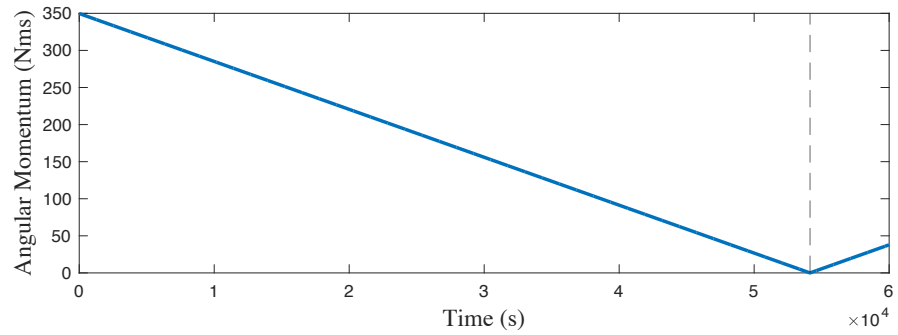

(b) Servicer angular momentum magnitude.

Figure 5. The behavior of the servicer's angular momentum when exposed to ${}^{\mathcal{B}}\boldsymbol{L}_e$ = [0.0052, 0.0039, 6.5e-5]$^{\mathrm{T}}$ Nm over 60,000s. The dashed line indicates the time where minimum angular momentum is achieved.

angular momentum is constant and it decreases/increases linearly, as shown in Fig. 5(b). When this is not the case, the net decreases in angular momentum magnitude is constantly varying, resulting in the parabolic shape shown by Fig. 6(b). The second major difference is the non-zero minimum value. It takes 32,010 s for the angular momentum of the servicer to reach a minimum value of 103.7 Nms. Even with dot product of -0.95, the angular momentum of the servicer can only be decreased by 246 Nms rather than the full 350 Nms. This occurs because when the X axis reaction wheel reaches a zero speed, the Y axis reaction wheel still has non-zero wheel speeds. At this point, the y-axis reaction wheel is still driving the change in angular momentum, but, once the X axis reaction reaches a critical point at 32,010 s, it becomes the dominate contribute and the angular momentum begins to increase. Even though the angular momentum of the servicer only partially decreases, the angular momentum of the spacecraft is still reduced using only electrostatic torques. While a perfectly anti-parallel torque is more effective, it is not required to perform significant momentum transfer with electrostatic torques.

Continuous Momentum Management with Target Having Fixed Relative Attitude

As opposed to the single momentum management maneuver, continuous momentum management has a spacecraft reduce its angular momentum repeatedly. This technique allows for charged spacecraft to maintain small separation distances without the concern of the constant electrostatic

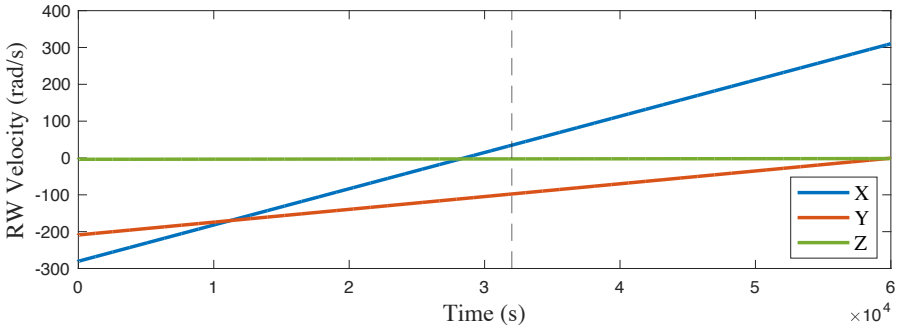

(a) Servicer reaction wheel velocities.

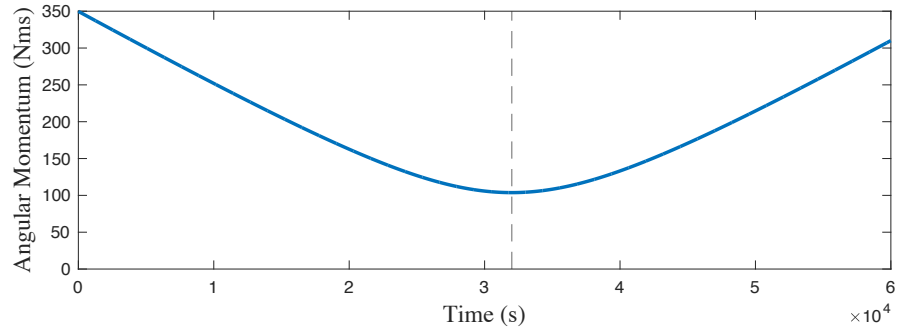

(b) Servicer angular momentum magnitude.

Figure 6. The behavior of the servicer's angular momentum when exposed to ${}^{\mathcal{B}}\boldsymbol{L}_e$ = [0.0098, 0.0035, 0.000032]$^{\mathrm{T}}$ Nm over 60,000s. The dashed line indicates the time where minimum angular momentum is achieved.

torque causing the reaction wheels to saturate. The spacecraft scenario for continuous momentum management is as follows: a servicing spacecraft with zero initial angular momentum is maintaining a desired attitude relative to a target. Because both spacecraft have large electric potentials, a significant electrostatic torque is generated between them, causing the servicer's reaction wheels to spin up. To avoid wheel speed saturation, once one of the reaction wheels reaches a designated speed threshold, the servicer computes the attitude that generates the opposite electrostatic torque and rotates to this new reference attitude. It maintains this attitude until the reaction wheel speed reaches zero, at which point the servicer rotates back to the original orientation. For these preliminary results, before the servicer preforms the attitude adjustment, the separation distance is increased to 100 m such that the electrostatic torques experienced during the rotations are negligible.

Figure 7 shows the two attitudes the servicer is switching between. It can be seen that, while the servicing attitude is the same as that in Fig. 3, the anti-torque attitude is not. This second anti-torque attitude corresponds to $\boldsymbol{\sigma}$ = (-1,0,0) and is chosen because it showcases the momentum management behavior best. At the servicing attitude, the generated electrostatic torque is ${}^{\mathcal{B}}\boldsymbol{L}_e$ = [0.0003, -0.0026, 0.0018] Nm. The electrostatic torque at the anti-torque attitude is ${}^{\mathcal{B}}\boldsymbol{L}_e$ = [1.3e-05, -0.0042, 0.0024] Nm.

While the servicer maintains the servicing attitude shown in Fig. 7(a), its reaction wheels spin up until they reach a designated threshold. The actual saturation point of reaction wheels can vary

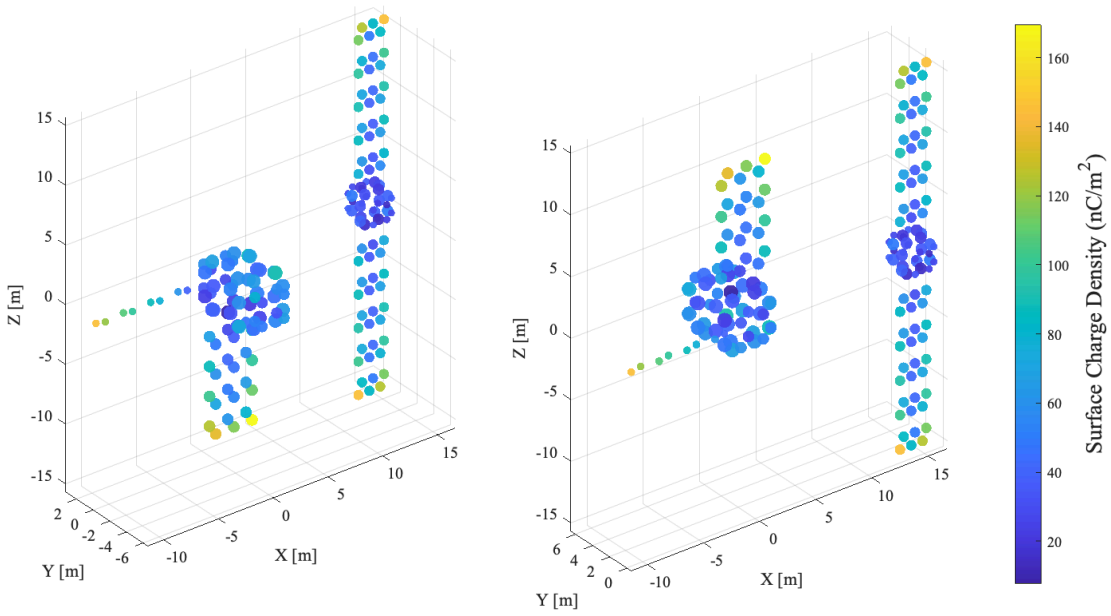

(a) The relative servicing attitude.

(b) The relative anti-torque attitude.

Figure 7. The MSM of the GOES-R and SSL-1300 spacecraft at the servicing and anti-torque attitudes used in the continuous momentum management maneuver simulations. There is a 15 m separation distance between the two spacecraft and they both have an electric potential of 10 kV.

significantly: for OCE reaction wheels, this speed can range from 126 rad/s to 681 rad/s.[29] For these simulations, a threshold of 50 rad/s and saturation speed of 100 rad/s are chosen. While most reaction wheels can safely operate at these wheel speeds, using this threshold reduces the simulation time and, other than the magnitude of the values, the behavior of the reaction wheels and angular momentum will be relatively unaffected. The goal of the threshold is to ensures that wheel speeds experienced during the maneuver do not jump above the breaking speed. Once one of the reaction wheel reaches 50 rad/s, the spacecraft rotates to the orientation shown in Fig. 7(b) and maintains this attitude until the same reaction wheel decreases by 50 ad/s, at which point it rotates back to the servicing attitude. Figure 8 shows the reaction wheel speeds and angular momentum magnitude over 200,000 seconds of these maneuvers.

From Fig. 8(a) , it can be seen that the reaction wheels perform multiple maneuvers over the course of the simulation. Every instance where the wheels speeds suddenly spike corresponds to a rotation. It takes approximately 20,000 s for the Y axis reaction wheel to reach a speed 50 rad/s. This makes sense as the largest torque is about the Y axis. After the first momentum transfer maneuver shown by the dashed line, it can be seen that, while their speeds have decreased, both the X and Z axis reaction wheels have not reached a zero velocity. This product of the control can also be seen in Fig. 8(b), where the angular momentum only decreases to 6.1 Nms. This trend of the Y axis reaction wheels reaching 50 rad/s first and the X and Z axis wheels not reaching zero continues, along with the ever increasing angular momentum, for the full 200,000 s. This momentum management does eventually fail as the non-perfectly anti-torques cause angular momentum to continually build up. After 259,300 s, the velocity of the X axis reaction wheel exceeds the 100 rad/s breaking velocity while rotating back to the servicing attitude. If this happened during a mission,

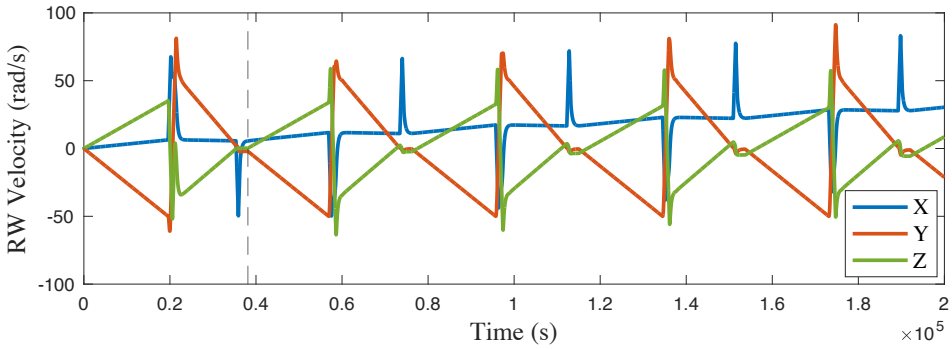

(a) Servicer reaction wheel velocities during multiple momentum management maneuvers.

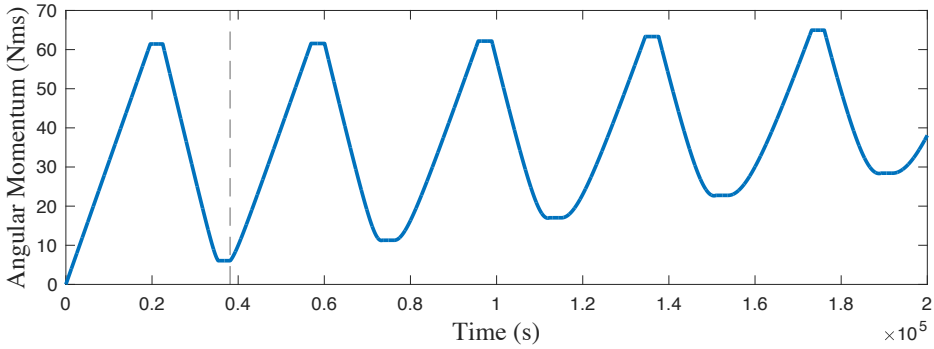

(b) Servicer angular momentum magnitude during multiple momentum management maneuvers.

Figure 8. The behavior of the servicer's angular momentum when using electrostatic torques to manage momentum while maintaining a servicing attitude over 200,000 s. The dashed line corresponds to the completion of the first maneuver.

the wheel would break and the spacecraft would no longer have 3 axis control. However, without this control, the Y axis reaction wheel would have exceeded the 100 rad/s maximum after 39,180 s. Instead, with the momentum management, the mission is extended to over 250,000 s and the amount of time spent at the servicer attitude increases to over 160,000 s, 4× longer.

CONCLUSION

The objective of this paper is to introduce the concept of using electrostatic torques for momentum management and present preliminary results demonstrating the feasibility of this technique. Using two charged spacecraft with a separation distance of 15 m, two momentum management scenarios are presented: a single maneuver with a fixed target and continuous management with a fixed target. In both cases, the speed of the reaction wheels, and therefore the angular momentum of the servicer, was significantly reduced using only electrostatic forces.

A single maneuver is explored fist. When the electrostatic torque is perfectly anti-parallel, the servicer is able to achieve an angular momentum of zero. If the electrostatic torque is not anti-parallel, the angular momentum of the servicer is still reduced, but cannot be driven to zero. The quality of the computed electrostatic torque, how anti-parallel it is, depends heavily on the search space being employed in the anti-torque finding function. In this paper, the database of attitudes

and electrostatic torques consists of one million values, but increasing the size of the data (increasing the discretization) can result in higher quality torques being found. This database only needs to be computed once for a given scenario; however, changing the separation distance, spacecraft geometries, or electric potential requires recomputing this database.

Repeatedly transferring momentum to the target is also explored. For this scenario, a target is switching between two attitudes: the servicing attitude and a momentum transfer attitude. The electrostatic torques experienced at these attitudes are in opposing directions. By switching between attitudes as the reaction wheel speeds increase, it is shown that the servicer's reaction wheels can be kept from reaching their breaking speed. This both extends the mission lifetime and increases the time spent at the servicing attitude. Additionally, because these torques are internal torques in relation to the 2 spacecraft system, when angular momentum of the servicer increases, that of the target decreases. This means, unlike the single maneuver where the target absorbs the angular momentum of the servicer, it is instead being "passed" back and forth between the two spacecraft. Because of this, if the perfect anti-parallel torque can be found, the momentum transfer maneuvers could continue indefinitely.

Throughout this paper, translational dynamics are not considered; therefore, a comparison between the fuel requirements to preform these maneuvers and the fuel required for using thrusters to dump angular momentum is not considered. However, the momentum transfer technique shown here functions outside of Earth's orbit, far away from its magnetic field where magnetorquers are ineffective, such as cislunar space. Additionally, the angular momentum storage capacity of the target is assumed to be large and that the change in its angular momentum of the target is negligible. However, this assumption only holds true for very large spacecraft like the ISS or Lunar Gateway. For small spacecraft, the increase in angular momentum could cause the target's reaction wheels to saturate during the maneuvers. The effect on the target's angular momentum and reaction wheels will be considered during the advancement of this research.

ACKNOWLEDGMENTS

This project was supported by the Department of Defense (DoD) through the National Defense Science and Engineering Graduate (NDSEG) Fellowship Program. Thank you to the Air Force Office of Scientific Research (AFOSR) for general support enabling Electrostatic Tractor research.

REFERENCES

[1] S. T. Lai, *Fundamentals of Spacecraft Charging*. Princeton University Press, Oct. 2011, 10.2307/j.ctvcm4j2n.

[2] K. Wilson and H. Schaub, "Impact of Electrostatic Perturbations on Proximity Operations in High Earth Orbits," *Journal of Spacecraft and Rockets*, Vol. 58, No. 5, 2021, pp. 1–10, 10.2514/1.a35039.

[3] K. Wilson and H. Schaub, "Constrained guidance for spacecraft proximity operations under electrostatic perturbations," *IEEE Aerospace Engineering Conference*, Big Sky, MT, Mar. 2021, pp. 1–11.

[4] K. Wilson, A. Romero Calvo, and H. Schaub, "Constrained Guidance for Spacecraft Proximity Operations Under Electrostatic Perturbations," *Journal of Spacecraft and Rockets*, Vol. 59, July–Aug. 2022, pp. 1304–1316, 10.2514/1.A35162.

[5] H. Schaub and D. F. Moorer, "Geosynchronous Large Debris Reorbiter: Challenges and Prospects," *The Journal of the Astronautical Sciences*, Vol. 59, Jun. 2012, pp. 161–176, 10.1007/s40295-013-0011-8.

[6] H. Schaub and Z. Sternovsky, "Active Space Debris Charging for Contactless Electrostatic Disposal Maneuvers," *Advances in Space Research*, Vol. 43, No. 1, 2014, pp. 110–118, dx.doi.org/10.1016/j.asr.2013.10.003.

[7] D. F. Moorer and H. Schaub, "Electrostatic spacecraft reorbiter," Feb. 2011. US Patent 8,205,838 B2.

[8] D. F. Moorer and H. Schaub, "Hybrid electrostatic space," Feb. 2011. US Patent 0036951-A1.

[9] H. Schaub and L. E. Z. Jasper, "Circular Orbit Radius Control Using Electrostatic Actuation for 2-Craft Configurations," *AAS/AIAA Astrodynamics Specialist Conference*, Girdwood, Alaska, July 31 – August 4 2011. Paper AAS 11–498.

[10] E. A. Hogan and H. Schaub, "Relative Motion Control For Two-Spacecraft Electrostatic Orbit Corrections," *Journal of Guidance, Control, and Dynamics*, Vol. 36, Jan. 2013, pp. 240–249, 10.2514/1.56118.

[11] H. Schaub and D. Stevenson, "Prospects of Relative Attitude Control Using Coulomb Actuation," *The Journal of the Astronautical Sciences*, Vol. 60, Dec. 2013, pp. 258–277, 10.1007/s40295-015-0048-y.

[12] T. Bennett and H. Schaub, "Contactless electrostatic detumbling of axi-symmetric GEO objects with nominal pushing or pulling," *Advances in Space Research*, Vol. 62, Dec. 2018, pp. 2977–2987, 10.1016/j.asr.2018.07.021.

[13] V. Aslanov and H. Schaub, "Detumbling Attitude Control Analysis Considering an Electrostatic Pusher Configuration," *Journal of Guidance, Control, and Dynamics*, Vol. 42, Apr. 2019, pp. 900–909, 10.2514/1.G003966.

[14] T. Bennett and H. Schaub, "Touchless Electrostatic Three-dimensional Detumbling of Large Axis-symmetric Debris," *The Journal of the Astronautical Sciences*, Vol. 62, Sep. 2015, pp. 233–253, 10.1007/s40295-015-0075-8.

[15] D. Stevenson and H. Schaub, "Electrostatic spacecraft rate and attitude control—Experimental results and performance considerations," *Acta Astronautica*, Vol. 119, Feb. 2016, pp. 22–33, 10.1016/j.actaastro.2015.10.023.

[16] E. A. Hogan and H. Schaub, "Three-Axis Attitude Control Using Redundant Reaction Wheels with Continuous Momentum Dumping," *AIAA Journal of Guidance, Control, and Dynamics*, Vol. 38, Oct. 2015, pp. 1865–1871, 10.2514/1.G000812.

[17] H. Schaub and J. L. Junkins, *Analytical Mechanics of Space Systems*. Reston, VA: AIAA Education Series, 4th ed., 2018, 10.2514/4.105210.

[18] K. Ü. Emri and O. Cihan, "Control allocation of a GEO satellite for station-keeping and momentum management by using thrusters and reaction wheels," *Avrupa Bilim ve Teknoloji Dergisi*, No. 26, 2021, pp. 374–382.

[19] J.-F. Trégouët, D. Arzelier, D. Peaucelle, C. Pittet, and L. Zaccarian, "Reaction wheels desaturation using magnetorquers and static input allocation," *IEEE Transactions on Control Systems Technology*, Vol. 23, No. 2, 2014, pp. 525–539.

[20] F. Giulietti, A. A. Quarta, and P. Tortora, "Optimal control laws for momentum-wheel desaturation using magnetorquers," *Journal of guidance, control, and dynamics*, Vol. 29, No. 6, 2006, pp. 1464–1468.

[21] Y. Yang, "Spacecraft attitude and reaction wheel desaturation combined control method," *IEEE Transactions on Aerospace and Electronic Systems*, Vol. 53, No. 1, 2017, pp. 286–295.

[22] J. Hammerl and H. Schaub, "Debris Attitude Effects on Electrostatic Tractor Relative Motion Control Performance," *AAS/AIAA Astrodynamics Specialist Conference*, Big Sky, MT, Aug. 2021, pp. 1–13.

[23] J. Hammerl and H. Schaub, "Effects of Electric Potential Uncertainty on Electrostatic Tractor Relative Motion Control Equilibria," *Journal of Spacecraft and Rockets*, Vol. 59, March – April 2022, pp. 552–562, 10.2514/1.A35165.

[24] D. Stevenson and H. Schaub, "Multi-Sphere Method for modeling spacecraft electrostatic forces and torques," *Advances in Space Research*, Vol. 51, Jan. 2013, pp. 10–20, 10.1016/j.asr.2012.08.014.

[25] D. Stevenson and H. Schaub, "Optimization of Sphere Population for Electrostatic Multi Sphere Model," *IEEE Transactions on Plasma Science*, Vol. 41, Dec. 2013, pp. 3526–3535, 10.1109/TPS.2013.2283716.

[26] G. Ingram, J. Hughes, T. Bennett, C. Reilly, and H. Schaub, "Volume Multi-Sphere-Model Development Using Electric Field Matching," *Journal of Astronautical Sciences*, Vol. 65, No. 4, 2018, pp. 377–399, 10.1007/s40295-018-0136-x.

[27] J. A. Hughes and H. Schaub, "Heterogeneous Surface Multisphere Models Using Method of Moments Foundations," *Journal of Spacecraft and Rockets*, Vol. 56, Jul. 2019, pp. 1259–1266, 10.2514/1.A34434.

[28] T. Marshall and M. Fletcher, "ACTUATORS: Meeting high-quality RWA commercial demand through innovative design," *8th European Space Mechanisms and Tribology Symposium* (D. Danesy, ed.), Vol. 438 of *ESA Special Publication*, Sept. 1999, p. 253.

[29] O.C.E Technology, "OCE Overview: Reaction Wheels," OCE-RW40 datasheet, July 2024.